MOLECULAR AND CELLULAR BIOLOGY, Apr. 2003, p. 2564–2576 Vol. 23, No. 7
0270-7306/03/$08.00+0 DOI: 10.1128/MCB.23.7.2564–2576.2003

Myeloid Cell Function in MRP-14 (S100A9) Null Mice

Josie A. R. Hobbs, Richard May,† Kiki Tanousis, Eileen McNeill, Margaret Mathies,‡ Christoffer Gebhardt,§ Robert Henderson, Matthew J. Robinson,¶ and Nancy Hogg*

Leukocyte Adhesion Laboratory, Cancer Research UK, London Research Institute, Lincoln's Inn Fields Laboratories, London WC2A 3PX, United Kingdom

Received 3 June 2002/Returned for modification 31 July 2002/Accepted 7 January 2003

Myeloid-related protein 14 (MRP-14) and its heterodimeric partner, MRP-8, are cytosolic calcium-binding proteins, highly expressed in neutrophils and monocytes. To understand the function of MRP-14, we performed targeted disruption of the MRP-14 gene in mice. MRP-14$^{-/-}$ mice showed no obvious phenotype and were fertile. MRP-8 mRNA but not protein is present in the myeloid cells of these mice, suggesting that the stability of MRP-8 protein is dependent on MRP-14 expression. A compensatory increase in other proteins was not detected in cells lacking MRP-8 and MRP-14. Although the morphology of MRP-14$^{-/-}$ myeloid cells was not altered, they were significantly less dense. When Ca^{2+} responses were investigated, there was no change in the maximal response to the chemokine MIP-2. At lower concentrations, however, there was reduced responsiveness in MRP-14$^{-/-}$ compared with MRP-14$^{+/+}$ neutrophils. This alteration in the ability to flux Ca^{2+} did not impair the ability of the MRP-14$^{-/-}$ neutrophils to respond chemotactically to MIP-2. In addition, the myeloid cell functions of phagocytosis, superoxide burst, and apoptosis were unaffected in MRP-14$^{-/-}$ cells. In an in vivo model of peritonitis, MRP-14$^{-/-}$ mice showed no difference from wild-type mice in induced inflammatory response. The data indicate that MRP-14 and MRP-8 are dispensable for many myeloid cell functions.

Neutrophils and monocytes are the first cells to migrate to infected or injured tissue, forming the initial response of the immune system. Myeloid cells are particularly well equipped to deal with bacterial infections because they can phagocytose microorganisms and kill them through induction of the respiratory burst (55). Additionally, myeloid cells synthesize and release cytokines, chemokines, and many other factors that influence immune responsiveness.

Among the most abundant proteins expressed by myeloid cells are MRP-8 (S100A8) and MRP-14 (S100A9), which, in humans, form a heterodimer constituting ≈45% of neutrophil and ≈1% of monocyte cytosolic proteins (9, 19, 31, 36). Human MRP-8 and MRP-14 are also constitutively expressed by secretory epithelia and can be induced in a broader range of epithelia, such as keratinocytes, following infections (11). MRP-8 and MRP-14 are members of the S100 family of Ca^{2+} binding proteins, which consists of 19 proteins, each with relatively cell type-specific expression (5, 14, 17). The majority of the S100 genes are tightly clustered together on chromosome 1q21 in humans and chromosome 3 in the mouse (45). S100 proteins contain two EF hand Ca^{2+} binding motifs with the second being classical and the first having an atypical 14-residue loop coordinating the Ca^{2+} ion. The abundance and Ca^{2+} binding ability of S100 proteins suggested that they might act as Ca^{2+} buffers, but more recent evidence that Ca^{2+} binding both induces conformational change and regulates function in S100 proteins indicates that these proteins function as Ca^{2+} sensors (1, 8, 16, 17).

Human MRP-8 and MRP-14 are detected extracellularly on the vasculature at inflammatory sites where myeloid cells migrate into tissues, suggesting that secretion of the proteins may influence leukocyte trafficking (21, 44). S100 proteins lack conventional signal sequences, and the mechanism by which they are released from cells is poorly understood. One report, however, suggests that the MRP proteins are secreted by monocytes through a tubulin-dependent mechanism (41). Several classes of MRP-8/MRP-14 receptors have been described recently, all of which are expressed by the vasculature. MRP-8 and MRP-14 have been shown to bind to CD36 (26), to special carboxylated N-glycans (50), and to heparin-like glycosaminoglycans (44). In addition, S100A12 (also called MRP-6 and EN-RAGE), which is closely related to MRP-14, binds to the scavenger receptor RAGE, which has a central role in inflammatory responses (20).

Extracellular functions associated with the immune response have been ascribed to several S100 proteins. Murine MRP-8, also called CP-10, has been characterized as a potent chemotactic factor for myeloid cells, with activity at 10^{-13} M (28, 29). Other family members, S100A12 (20), psoriasin (S100A7) (25), and S100L (S100A2) (27), have also been reported to be chemotactic but have been less extensively characterized. MRP-14 differs from other S100 proteins in having an extended C-terminal sequence of 23 residues which is identical to a factor described as having migration-inhibitory activity for human myeloid cells (10). Whether the S100 proteins act to promote

* Corresponding author. Mailing address: Leukocyte Adhesion Laboratory, Cancer Research UK, London Research Institute, Lincoln's Inn Fields Laboratories, London WC2A 3PX, United Kingdom. Phone: 44 20 7269 3255. Fax: 44 20 7269 3093. E-mail: nancy.hogg@cancer.org.uk.

† Present address: Cambridge Antibody Technology, Melbourn SG8 6JJ, United Kingdom.

‡ Present address: W. M. Keck Science Center, The Claremont Colleges, Claremont, CA 91711.

§ Present address: Division of Signal Transduction and Growth Control, German Cancer Research Centre, 69120 Heidelberg, Germany.

¶ Present address: Immune Cell Biology, National Institute of Medical Research, Mill Hill, London NW7 1AA, United Kingdom

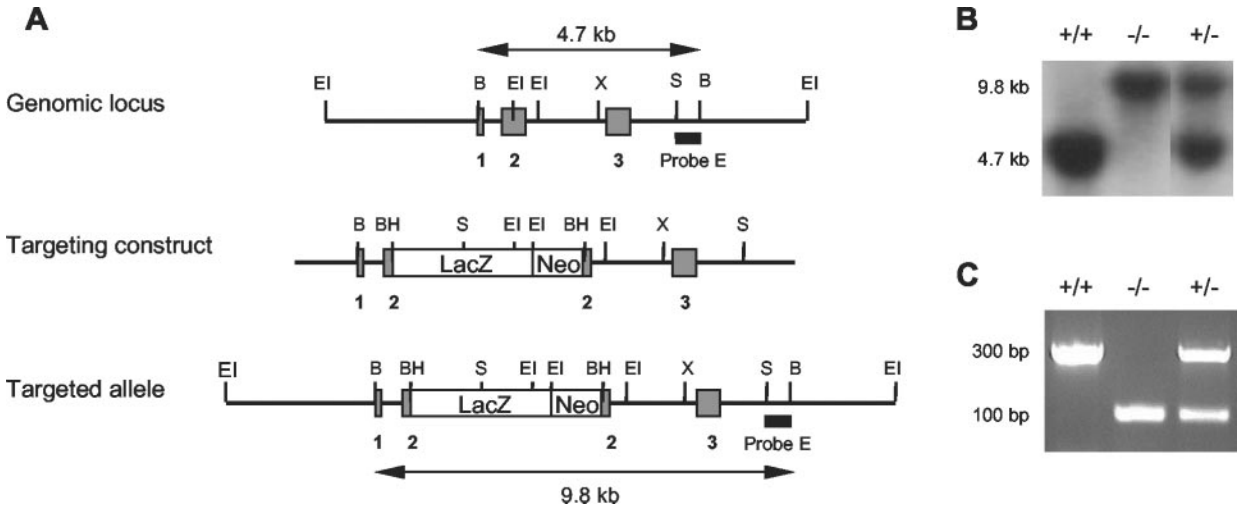

FIG. 1. Targeted inactivation of the *MRP-14* gene. (A) The murine *MRP-14* gene consists of three exons (grey bars). Disruption of the *MRP-14* gene was achieved by insertion of the *lacZ-neo* cassette into exon 2 immediately following the transcriptional start site. BH, *Bam*HI; B, *Bgl*II; EI, *Eco*RI; S, *Sac*I; X, *Xba*I. (B) Southern hybridization analysis of mouse tail DNA digested with *Bgl*II and hybridized with probe E. (C) Ethidium bromide-stained 1.8% agarose gel of PCR products generated from amplified mouse tail DNA.

or prevent cell migration is therefore a key issue. MRP-8 also appears to be required for embryo development, as *MRP-8* gene deletion has been reported to cause lethality by day 9.5 of murine development (38).

In humans, MRP-8 and MRP-14 exist as both heterodimers and higher-order complexes (9, 24, 51). In the mouse, there is evidence that MRP-8 and MRP-14 exist separately (28, 40). In spite of these differences, mouse and human MRP-14 are considered functionally homologous proteins (34, 40). In order to gain insight into the physiological role of MRP-14, we generated MRP-14$^{-/-}$ mice and focused our investigation on examining the functions of myeloid cells deficient in this protein. Surprisingly, MRP-14 appears to be dispensable for many important calcium-dependent aspects of myeloid cell function.

MATERIALS AND METHODS

Disruption of *MRP-14* gene. A comparison of the murine (31) and human (36) *MRP-14* cDNA sequences with the human *MRP-14* genomic sequence (30), coupled with the information that genomic structure is conserved across species in this gene family (42), allowed prediction of the probable intron and exon boundaries of the murine *MRP-14* gene. A 230-bp PCR-generated product from murine exon 3 was used to probe a murine 129Sv genomic library. A lambda phage clone containing 10.8 kb of the *MRP-14* gene in three *Eco*RI fragments of 4, 0.3, and 6.5 kb from 5′ of exon 1 to 3′ of exon 3 was isolated (see Fig. 1). A selection cassette containing stop codons in all three reading frames and containing the *lacZ*/*neo* sequence was targeted to a unique *Bam*HI site introduced immediately following the ATG start codon in exon 2.

Electroporated GK 129 embryonic stem (ES) cell clones containing a single targeted allele were identified by Southern analysis with probe E, a 650-bp *Sac*I-*Bgl*II restriction fragment located immediately 3′ of the targeting construct. *Bgl*II digests of wild-type and mutant alleles yielded probe E-hybridizing fragments of 4.7 kb and 9.8 kb, respectively. Correctly targeted ES cell clones were injected into C57BL/6 mouse blastocysts. Chimeric mice and subsequent 129Sv × C57BL/6 backcross generations were genotyped by Southern hybridization with probe E.

Alternatively, PCR genotyping was performed with the oligonucleotide primers GF1 (AACATCTGTGACTCTTTAGCC), GB1 (CATCTGAGAAGGTGC TTTGTT), and GNeo (ACCGCTTCCTCGTGCTTTACG). PCR of the wild-type allele produced a 300-bp product, whereas PCR of the mutant allele produced a 100-bp product. The reported experiments were carried out on two independently derived strains of MRP-14$^{-/-}$ and MRP-14$^{+/+}$ littermate mice of backcross generation 3 to 5. The mice were maintained under specific-pathogen-free conditions and in accordance with United Kingdom Home Office regulations.

Myeloid cell preparation. Murine bone marrow leukocytes were harvested by flushing both femurs and tibiae with the relevant assay buffer. Erythrocytes were lysed with 0.144 M NH_4Cl–0.017 M Tris-HCl, pH 7.2.

MRP-specific antibodies. Rat monoclonal antibody (MAb) 2B10 (immunoglobulin G2a [IgG2a]) was derived from an immunization with recombinant full-length murine MRP-14 (R. May, unpublished data). MAb 2B10 does not react with MRP-8, human MRP-6, -8, or -14 proteins, or S100B protein (data not shown). In flow cytometric assays, fluorescein isothiocyanate (FITC)-conjugated MAb 2B10 was tested with a comparably FITC-conjugated rat IgG2a isotype control MAb. Rabbit anti-MRP-8 was raised against synthesized full-length murine MRP-8 and was specific for MRP-8 when tested as described above (data not shown).

Immunohistochemistry. Sections (4 μm) were cut from paraffin-imbedded tissues and microwaved for 10 min at 700 W. Sections were then stained with rat MAb 2B10 and the IgG2a isotype control (10 μg/ml) in Tris-buffered saline, pH 7.6, for 40 min at room temperature, followed by biotinylated rabbit anti-rat Ig (1:100, Vector Laboratories) for 40 min at room temperature, and then StreptABComplex-horseradish peroxidase was used according to the manufacturer's instructions (Dako Ltd.), and finally, the sections were exposed to 0.5 mg of 3,3′-diaminobenzidine per ml for 2 to 3 min. Slides were counterstained in Harris' hematoxylin.

Flow cytometry. Bone marrow leukocytes or peritoneal lavage cells were suspended in FACSwash (phosphate-buffered saline containing 0.2% bovine serum albumin). Leukocytes were subjected to double immunostaining with MAbs 7/4 (Caltag Medsystems) and Gr-1 (BD Biosciences) in order to distinguish neutrophils (7/4 high, Gr-1 high) and monocytes (7/4 high, Gr-1 intermediate) (R. Henderson, unpublished data). The cells were either incubated with phycoerythrin (PE)-7/4 (1:20) and FITC–Gr-1 (1:200) for 20 min or stained with biotin–Gr-1 (1:50, Pharmingen) and then stained with peridinin chlorophyll protein-streptavidin (1:200, BD Biosciences) and PE-7/4 (1/20). To label cytosolic MRP-14, the cells were fixed with 4% formaldehyde, permeabilized with 0.5% saponin, and then labeled with MAb FITC-2B10 and control MAb FITC-IgG2a (both at 5 μg/ml).

To identify individual classes of blood leukocytes, 50 μl of blood was incubated with 50 μl of saturating antibody solution (FITC–Gr-1, FITC-B220, PE-NK1.1, PE-CD4, FITC-CD8 [BD Biosciences], or PE-7/4) for 30 min at room temperature. Cells were washed in FACSwash, and erythrocytes were lysed with FACSlysing solution (BD Biosciences) according to the manufacturer's instructions. Absolute cell counting was performed by adding a known quantity of calibration beads (CaliBrite; BD Biosciences) to a known sample volume as previously described (23). All flow cytometry experiments were carried out with a FACSCalibur (Becton Dickinson).

RNA isolation and RNase protection assay. Bone marrow cells were lysed, and extraction of RNA, probe preparation, and RNase protection assays were performed as described before (22). The probes corresponded to the full-length cDNA sequences of murine MRP-8 (343 bp, coding for residues 1 to 89) and MRP-14 (488 bp, coding for residues 1 to 113) and served as templates for the generation of ^{32}P-labeled antisense riboprobes. A glyceraldehyde-3-phosphate dehydrogenase probe was used as a control.

In situ hybridization. Specific localization of the mRNA for MRP-8 was accomplished by in situ hybridization with antisense riboprobes. The template for the MRP-8 riboprobe synthesis was identical to that used for the RNase protection assay (see above). cRNA probe labeled with [^{35}S]UTP (≈800 Ci/mmol; Amersham) was prepared as a runoff transcript from *Hin*dIII-linearized plasmid with T7 RNA polymerase. An antisense β-actin probe was used as a control. All in situ hybridization was performed on 4-μm serial sections of formalin-fixed, paraffin-embedded embryonic tissue at 6.5, 7.5, and 14 days post coitum (d.p.c.). The methods for treatment, hybridization, washing, and dipping of slides in photographic emulsion for autoradiography were described previously (47). Autoradiography was carried out at 4°C for 7 or 10 days before developing and counterstaining with Giemsa stain.

Two-dimensional isoelectric focusing and sodium dodecyl sulfate-polyacrylamide gel electrophoresis. Bone marrow leukocytes (10^8/ml) were lysed in 8 M urea–4% CHAPS (3-[(cholamidopropyl)-dimethylammonio]-1-propanesulfonate)–40 mM Tris base containing Complete EDTA-free protease inhibitor cocktail (Roche) for 1 h at room temperature, followed by 1:4 lysate dilution in 8 M urea–2% CHAPS–5% glycerol–65 mM dithiothreitol–0.5% immobilized pH gradient buffer. The lysate was separated by isoelectric focusing with an immobilized pH gradient (IPGphor) 18-cm strip with a linear pH range of 3 to 10, according to the manufacturer's protocol (Amersham Pharmacia Biotech). The strips were then transferred onto a vertical sodium dodecyl sulfate–17.5% polyacrylamide gel. Protein spots were visualized with colloidal Coomassie blue. Two groups of four MRP-14$^{+/+}$ and four MRP-14$^{-/-}$ bone marrow lysates were compared with PDQuest two-dimensional gel analysis software (Bio-Rad, version 6.2). A total of 175 proteins were analyzed on each of the eight gels. The Mann-Whitney test was used to test for proteins that had been significantly altered between the groups.

Western blotting. Western blotting was carried out on bone marrow cell lysates, separated by sodium dodecyl sulfate–17.5% polyacrylamide gel electrophoresis and followed by transfer to nitrocellulose. MRP-14 was detected with MAb 2B10 (2 μg/ml) and compared to control IgG2a, followed by goat anti-rat immunoglobulin-horseradish peroxidase conjugate (1:500, Southern Biotechnology). MRP-8 was detected with rabbit anti-MRP-8 (1:1,000) and compared with control rabbit serum, followed by goat anti-rabbit immunoglobulin-horseradish peroxidase conjugate (1:10,000; Dako Ltd.).

Leukocyte density analysis. A 1.097-g/ml solution of isoosmotic Percoll in 0.15 M NaCl (Amersham Pharmacia Biotech) was prepared and used to create a 9-ml self-generating continuous gradient as described by the manufacturer (running conditions: 23° angle-head rotor, 30,000 × *g*, 25°C, 12 min). The gradient was calibrated between 1.018 and 1.138 g/ml with density marker beads (Amersham Pharmacia Biotech). Bone marrow leukocytes at 5×10^7/ml in Hanks' balanced salt solution (Sigma Aldrich) were layered onto the preformed gradient at 1 ml/tube and centrifuged at 700 × *g* at 21°C for 30 min. The mean buoyant density of the cellular bands was calculated with density marker bead calibration, and the composition was determined by flow cytometric analysis as described above.

Measurement of intracellular calcium. Bone marrow leukocytes (10^7/ml in Hanks' balanced salt solution, 1 mM Ca^{2+}, 0.5% bovine serum albumin) were loaded with indo-1-acetoxymethyl ester (Indo-1; Cambridge Bioscience) at 30°C as described before (32). Cells were then stained with MAbs PE-7/4 and FITC–Gr-1 and maintained at 30°C prior to use. Intracellular calcium was monitored with a BD LSR flow cytometer (FL-4 530/30-nm BF filter, FL-5 424/44-nm BF filter; Becton Dickinson). Stimuli used were MIP-2 (Peprotech) and ionomycin (Calbiochem). Data were analyzed with FlowJo software (Tree Star Inc.).

Leukocyte chemotaxis assay. Bone marrow leukocytes (5×10^6/ml in Hanks' balanced salt solution, 10 mM HEPES, 1 mM Ca^{2+}, 0.2% bovine serum albumin) were added to Transwell plates according to the manufacturer's instructions (3-μm pore; Corning). Cells were allowed to migrate for 2 h at 37°C towards MIP-2 (Peprotech) at 0.1 to 500 ng/ml or towards medium alone. The number of neutrophils and monocytes that migrated was determined by flow cytometry as described above.

Measurement of neutrophil superoxide production. The production of superoxide was measured as described before (49). Briefly, bone marrow leukocytes (2×10^6/ml in Hanks' balanced salt solution) were labeled with 0.1 μM dihydrorhodamine 123 (Cambridge Bioscience) for 5 min at 37°C prior to stimulation with phorbol-12,13-dibutyrate (PDBu; Calbiochem) at 50 to 200 nM for 30 min. The superoxide production of neutrophils and monocytes was analyzed by flow cytometry.

Phagocytosis. Bone marrow leukocytes (6×10^5 in 150 μl of Dulbecco's modified Eagle's medium–10% fetal bovine serum) were combined with 150 μl of reconstituted fluorescein conjugated *Escherichia coli* K-12 particles (Molecular Probes) and incubated at 37°C. At time points between 0 and 8 h, the fluorescence of extracellular bacteria was quenched by adding trypan blue dye as described previously(54). Neutrophil and monocyte phagocytosis was analyzed by flow cytometry as described above.

Apoptosis. Bone marrow leukocytes (2.5×10^6/ml in Dulbecco's modified Eagle's medium–10% fetal bovine serum) were incubated at 37°C together with either 1 μM ionomycin (Calbiochem) or 2.5 μM thapsigargin (Calbiochem). At time points from 0 to 8 h, cells were stained with MAbs PE-7/4 and FITC–Gr-1 and resuspended in phosphate-buffered saline containing 0.1 μM LDS 751 (Exciton) for 20 min. 4′,6′-Diamidino-2-phenylindole (DAPI; Sigma-Aldrich) was added to a final concentration of 0.1 μg/ml, and samples were analyzed with a BD LSR flow cytometer (Becton Dickinson).

Thioglycolate-induced peritonitis. Peritonitis was induced in twelve to twenty-week-old mice by intraperitoneal injection of thioglycolate (3% [wt/vol] in 0.5 ml of sterile saline; Sigma Aldrich), as described elsewhere (18). At various time points up to 72 h, peritoneal cavities were lavaged, leukocytes in the lavage fluid were counted, and the proportions of neutrophils, monocytes, and other leukocytes were determined by flow cytometry as described above. Six to eight mice of each genotype were analyzed at each time point.

RESULTS

Generation of MRP-14-deficient mice. The *MRP-14* gene was disrupted in ES cells with a replacement-type targeting vector and the strategy shown in Fig. 1A. ES cells were electroporated, and of 196 neomycin (G418)-resistant clones, 13 were correctly targeted. Two targeted clones were injected into C57BL/6 mouse blastocysts, and two independent strains of MRP-14$^{-/-}$ mice were established. The *MRP-14* wild-type and mutant alleles were distinguished both by Southern hybridization with probe E following *Bgl*II digestion of mouse tail DNA (Fig. 1B) and by a PCR-based assay (Fig. 1C).

Interbreeding of MRP-14 heterozygotes yielded the proportions of 1.0:1.9:1.0 for wild-type–heterogeneous–null mice, approximating the expected ratio for Mendelian inheritance. The MRP-14$^{-/-}$ mice, which were maintained in specific-pathogen-free conditions, had no detectable tissue or organ abnormalities and lived a normal life span.

The liver, kidney, large and small intestine, skin, thymus, peripheral lymph nodes, and spleen from MRP-14$^{+/+}$ and MRP-14$^{-/-}$ mice were examined by immunochemistry with MAb 2B10. Positive MRP-14 staining was restricted to myeloid cells and most readily observed in spleen sections of MRP-14$^{+/+}$ mice (Fig. 2A and C). No staining was evident in the spleen sections of MRP-14$^{-/-}$ mice (Fig. 2B). The basic organization of the spleen is similar in MRP-14$^{+/+}$ and MRP-14$^{-/-}$ mice, and similar numbers of myeloid cells were found in spleens from both types of mice (data not shown).

Lack of MRP-14 expression in MRP-14$^{-/-}$ monocytes and neutrophils. In order to determine the expression levels of MRP-14 in neutrophils and monocytes from MRP-14$^{+/+}$ and MP-14$^{-/-}$ mice, a flow cytometry-based method was developed (R. Henderson, unpublished data). Bone marrow neutrophils and monocytes from MRP$^{+/+}$ and MRP-14$^{-/-}$ mice express the epitope recognized by MAb 7/4 at similar high levels (Fig. 3A). In MRP-14$^{+/+}$ mice, the MAb 7/4-positive population was composed of two subsets of cells (R2 and R3) expressing different levels of MRP-14 (Fig. 3B). These populations corresponded to monocytes (R2, low MRP-14) and

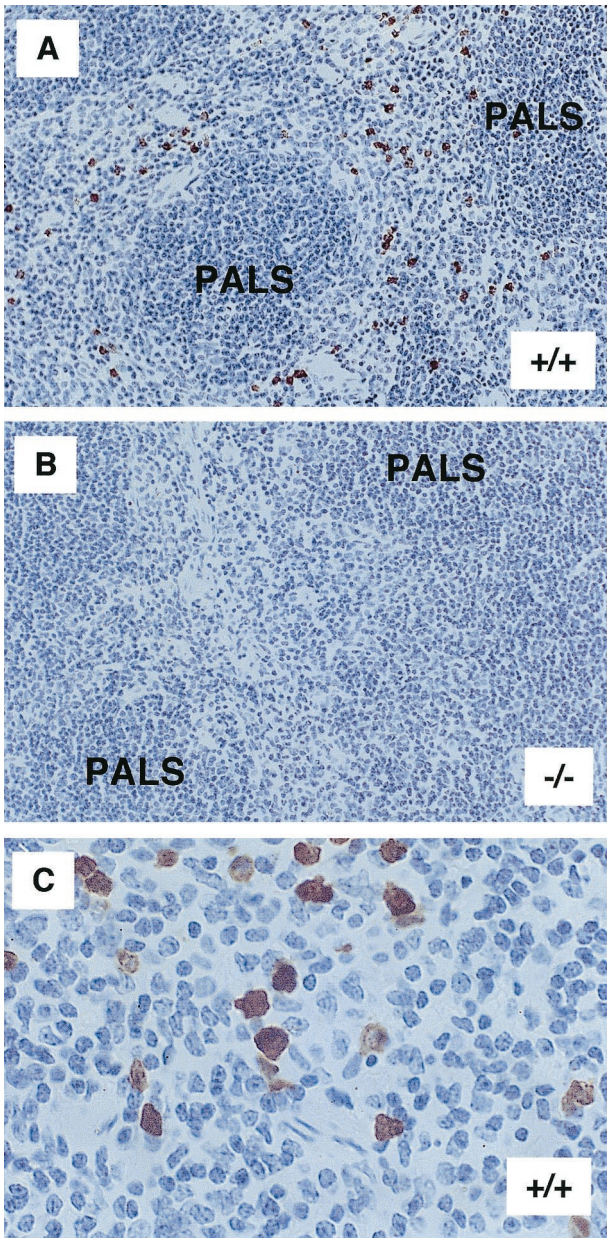

FIG. 2. Tissue sections of spleen from MRP-14$^{+/+}$ and MRP-14$^{-/-}$ mice. (A) MRP-14$^{+/+}$ spleen section showing positive staining of MRP-14-expressing myeloid cells scattered within the red pulp area with MAb 2B10. PALS, periarteriolar lymphoid sheath. (B) Spleen section from an MRP-14$^{-/-}$ mouse lacking MRP-14-positive staining with MAb 2B10. (C) Higher magnification of spleen from an MRP-14$^{+/+}$ mouse showing both moderate (monocyte) and strong (neutrophil) staining of myeloid cells.

neutrophils (R3, high MRP-14), as demonstrated by their forward and side scatter profiles (data not shown) and their differential staining with MAb Gr-1 (Fig. 3C). The same two classes of myeloid cells were also labeled in a comparable manner with MAb 2B10 when murine blood and spleen were examined (data not shown). In MRP-14$^{-/-}$ mice, monocytes and neutrophils failed to stain positively with MAb 2B10 (see overlap with control IgG2a MAb [R1] in Fig. 3B, lower histogram).

Absence of MRP-8 protein but not *MRP-8* mRNA in MRP-14-null neutrophils. Bone marrow cells were analyzed for expression of *MRP-14* as well as *MRP-8* mRNA (Fig. 4A). RNase protection assays demonstrated the absence of *MRP-14* mRNA in MRP-14$^{-/-}$ mice and, as expected, normal levels of *MRP-8* mRNA. The expression of a truncated form of MRP-14 was ruled out by reverse transcription -PCR with primers that amplified exon 3 in MRP-14$^{+/+}$ but not MRP-14$^{-/-}$ mice (data not shown). The absence of MRP-14 protein in bone marrow cells from MRP-14$^{-/-}$ mice was demonstrated by Western blotting with MAb 2B10 (Fig. 4B). The MAb 2B10 staining conditions were such that MRP-14 protein was not detectable in the MRP-14$^{-/-}$ cells at even when used at >256 times the amount used for the MRP-14$^{+/+}$ cells (data not shown).

Although *MRP-8* mRNA expression appeared normal in the RNase protection assay, no MRP-8 protein was detected in MRP-14$^{-/-}$ cells by Western blot analysis with an MRP-8-specific polyclonal antibody (Fig. 4B). MRP-8 protein was not detectable in MRP-14$^{-/-}$ cells even when the antibody was used at >100 times the amount used for wild-type lysates (data not shown).

Finally, we compared MRP-14$^{+/+}$ and MRP-14$^{-/-}$ bone marrow lysates by two-dimensional gel analysis. The only proteins that were significantly altered out of 175 proteins that were examined corresponded to MRP-8 and MRP-14, both of which were missing in MRP-14$^{-/-}$ lysates (Fig. 4C). These data were confirmed by Western blot analysis of the two-dimensional gels (data not shown). Two-dimensional gel analysis also did not reveal any obvious compensatory increases in other proteins which might balance the loss of MRP-8 and MRP-14, nor was there an overall general increase in protein content to compensate for the loss of the specific MRP proteins (Fig. 4C and data not shown). Furthermore, using reverse transcription-PCR, we could detect no alterations in bone marrow expression of S100A1 (7) or S100A4 (15), which are expressed generally by leukocytes (data not shown).

Expression of *MRP-8* mRNA during embryonic development in MRP-14$^{-/-}$ mice. MRP-8 has been reported to be expressed between days 6.5 and 8.5 of embryonic development (6.5 to 8.5 d.p.c.), and lack of MRP-8 has been shown to cause embryonic lethality by 9.5 d.p.c. in MRP-8$^{-/-}$ mice (38). The absence of MRP-8 protein in the myeloid cells of MRP-14$^{-/-}$ mice raised the issue of how these mice could be viable. We therefore performed in situ hybridization on MRP-14$^{+/+}$ and MRP-14$^{-/-}$ embryos to look for the expression of *MRP-8* mRNA. In agreement with Passey et al., we observed extensive MRP-8 expression at 6.5 d.p.c. (data not shown) and 7.5 d.p.c. in MRP-14$^{+/+}$ sections (Fig. 5A and B). In MRP-14$^{-/-}$ sections, *MRP-8* mRNA had the same localization pattern as in the MRP-14$^{+/+}$ sections, but the expression levels were substantially diminished (Fig. 5E and F). The *MRP-8* mRNA was localized to the maternal decidual tissue in both MRP-14$^{+/+}$ and MRP-14$^{-/-}$ sections. By 14 d.p.c., MRP-8 was detected exclusively in myeloid cells in the liver of a control C57BL/6 embryo (Fig. 5D). As a positive control, β-actin showed a wide distribution of staining in both embryonic and maternal tissues (Fig. 5C and G).

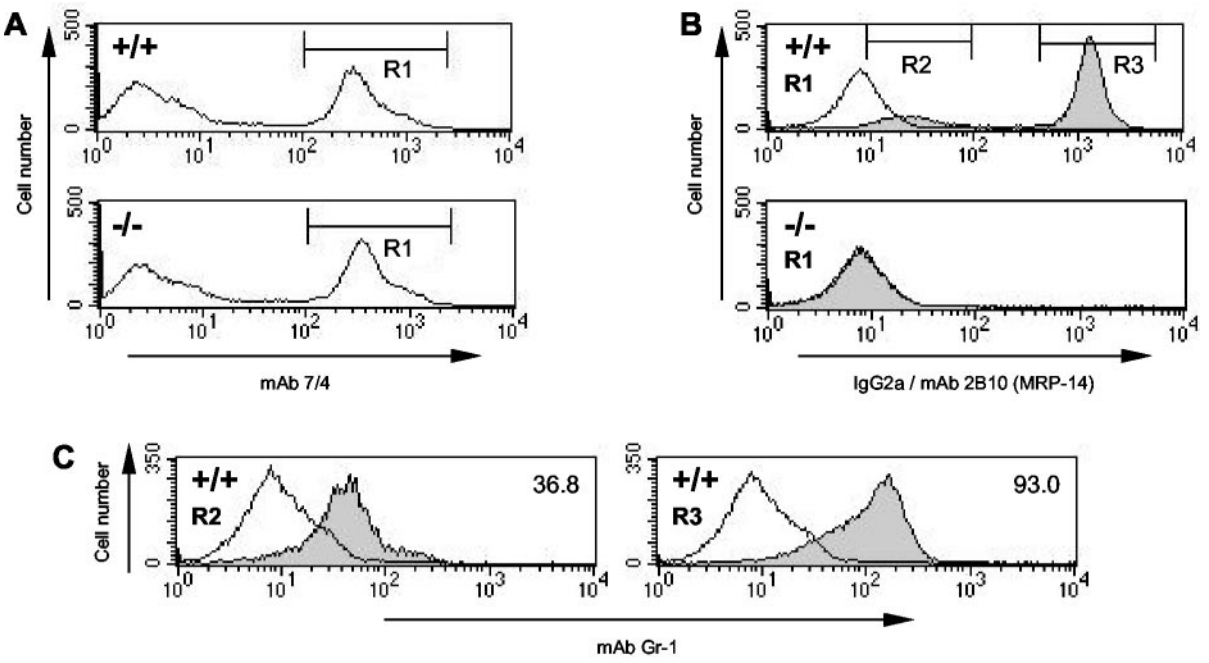

FIG. 3. MRP-14 protein is absent in MRP-$14^{-/-}$ monocytes and neutrophils. (A) Myeloid cells were identified by flow cytometry by staining MRP-$14^{+/+}$ and MRP-$14^{-/-}$ bone marrow cells with MAb 7/4. (B) The MAb 7/4-positive myeloid cells (R1) from MRP-$14^{+/+}$ and MRP-$14^{-/-}$ mice were intracellularly stained with either MAb 2B10, specific for MRP-14 (shaded histogram), or an IgG2a isotype control MAb (open histogram). (C) In MRP-$14^{+/+}$ mice, two different MRP-14-positive populations (R2 and R3) can be seen that are absent in MRP-$14^{-/-}$ myeloid cells. These populations correspond to monocytes (R2) and neutrophils (R3), based on their differential staining with MAb Gr-1. Open histogram represents the Gr-1-negative, 7/4-negative cells. Inset numbers represent the geometric mean fluorescence of three Gr-1-positive populations.

Normal numbers and morphology but difference in density of MRP-$14^{-/-}$ myeloid cells. The absence of both MRP-8 and MRP-14 had no significant effect on the number of circulating neutrophils or monocytes (Fig. 6A). The numbers of circulating CD4 and CD8 T lymphocytes, B lymphocytes, and NK cells were also unaffected (Fig. 6A). Furthermore, there were no obvious ultrastructural differences between MRP-$14^{+/+}$ and MRP-$14^{-/-}$ neutrophils (Fig. 6B) and monocytes (data not shown) by transmission electron microscopy of either peripheral blood- or bone marrow-derived cells (data not shown).

The density of neutrophils from MRP-$14^{+/+}$ and MRP-$14^{-/-}$ mice was measured by Percoll density gradient centrifugation. Two distinct bands were observed in processed gradients from both types of mice. An upper, less dense band with a mean buoyant density of 1.0439 g/ml was present in both MRP-$14^{+/+}$ and MRP-$14^{-/-}$ samples. This band consisted of ≈5% total neutrophils. The second, denser cellular band had a lower mean buoyant density in the MRP-$14^{-/-}$ samples (1.0811 g/ml) in comparison with the MRP-$14^{+/+}$ samples (1.0836 g/ml). This band was found to contain ≈80% of the total number of neutrophils loaded onto the gradient in both the MRP-$14^{+/+}$ and MRP-$14^{-/-}$ samples. Thus, there was a significant difference of 2.5 mg/ml in density between MRP-$14^{+/+}$ and MRP-$14^{-/-}$ neutrophils.

Calcium responses in MRP-$14^{-/-}$ neutrophils. To test whether the loss of such major calcium-binding proteins had an impact on intracellular calcium signaling, we investigated calcium flux induced in bone marrow neutrophils. Cells were loaded with Indo-1 dye, and neutrophils were identified by staining with MAbs 7/4 and Gr-1. Calcium-induced fluorochromatic changes were measured by flow cytometry. The basal level of intracellular Ca^{2+} was consistently higher in MRP-$14^{-/-}$ neutrophils than in wild-type cells (Fig. 7A). The chemokine MIP-2 produced a Ca^{2+} flux in wild-type and MRP-$14^{-/-}$ neutrophils from a threshold level of 0.1 ng/ml to a peak response at 5 and 10 ng/ml. At maximal doses of MIP-2, the levels of intracellular calcium in MRP-$14^{+/+}$ and MRP-$14^{-/-}$ neutrophils were identical, but at lower concentrations of stimulant, the response of MRP-$14^{-/-}$ neutrophils was significantly diminished (Fig. 7A and B). For example, the average change in intracellular calcium levels produced by 1 ng of MIP-2 per ml in MRP-$14^{-/-}$ neutrophils was 40% lower than that seen in MRP-$14^{+/+}$ cells (Fig. 7B). The rate of decay of the calcium transients was similar for MRP-$14^{+/+}$ and MRP-$14^{-/-}$ neutrophils. Maximal responses to the Ca^{2+} ionophore ionomycin (Fig. 7C) and the Ca^{2+} mobilizer thapsigargin (data not shown) were similar for MRP-$14^{+/+}$ and MRP-$14^{-/-}$ neutrophils in the absence and presence of extracellular calcium (data not shown).

Effect of *MRP-14* deletion on neutrophil function in vitro. To test whether the lack of MRP-8 and MRP-14 resulted in defects in any key neutrophil activities, a number of in vitro functional assays were performed. The ability of neutrophils to migrate from the vasculature into tissue was modeled in vitro with the Transwell chemotaxis assay. Migration of neutrophils to the CXC chemokine MIP-2 was unaffected by the absence of MRP-14 over a MIP-2 concentration range from 0.1 to 500 ng/ml, and MRP-$14^{+/+}$ and MRP-$14^{-/-}$ neutrophils showed a similar bell-shaped curve of responsiveness (Fig. 8A). There was also no difference in the chemotactic response to MIP-2

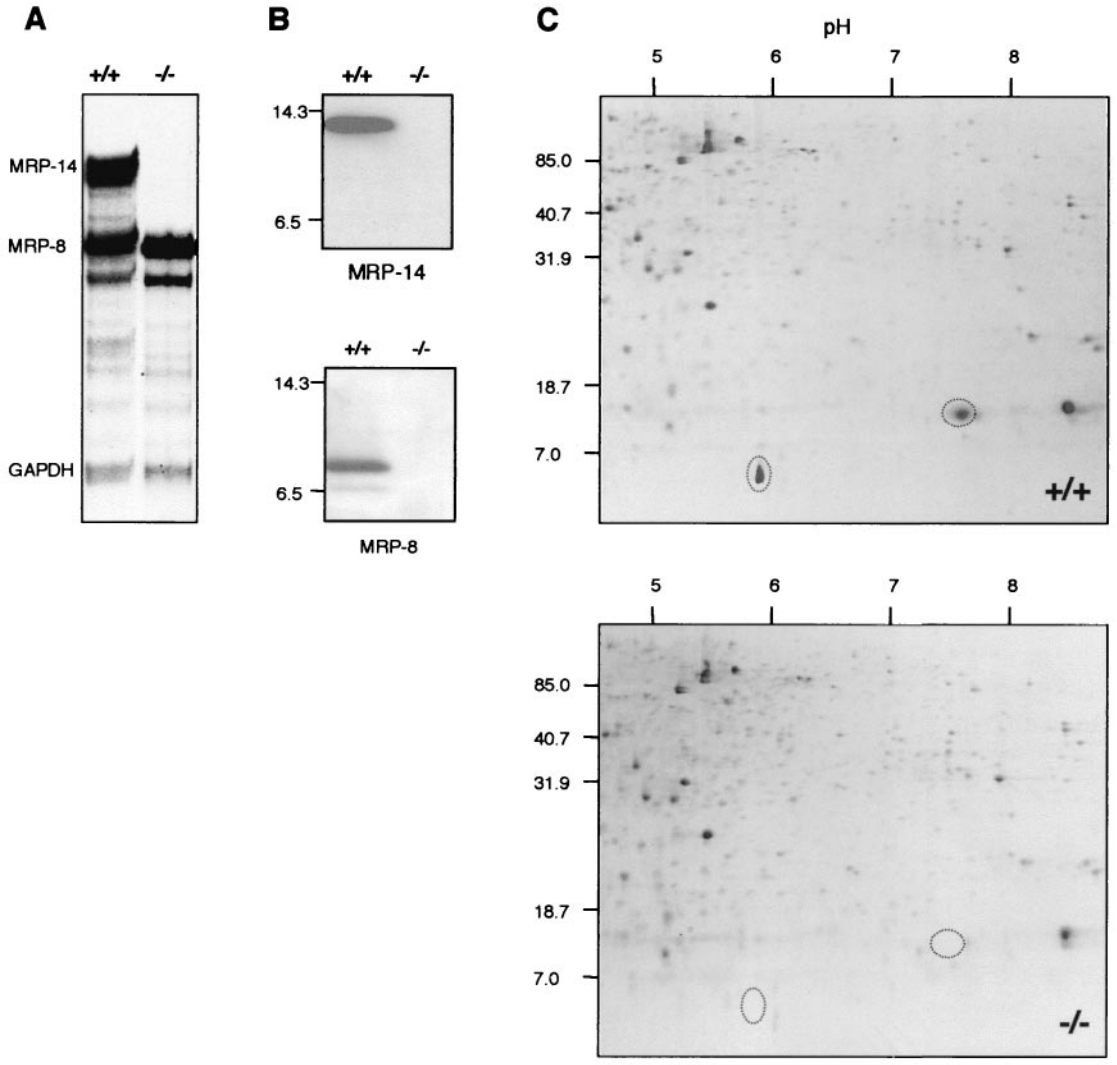

FIG. 4. *MRP-14* mRNA and both MRP-14 and MRP-8 proteins are absent in MRP-14$^{-/-}$ mice. (A) RNase protection assay ($n = 3$) showing the absence of *MRP-14* mRNA but the presence of *MRP-8* mRNA in MRP-14$^{-/-}$ mice. Glyceraldehyde-3-phosphate dehydrogenase (GAPDH) was used as a control. (B) Western blot analysis of bone marrow cell lysate stained with MAb 2B10 (MRP-14) and rabbit anti-MRP-8. Molecular size markers lysozyme (14.3 kDa) and aprotinin (6.5 kDa) are shown ($n = 5$). (C) Two-dimensional gel analysis showing absence of MRP-14 and MRP-8 proteins in MRP-14$^{-/-}$ bone marrow cells and lack of compensatory increase in other proteins ($n = 5$). Molecular size markers are shown in kilodaltons.

when cells migrated across a tumor necrosis factor alpha-stimulated bEND5 endothelial cell monolayer (data not shown).

The induction of the respiratory burst was tested by evaluating the ability of reactive oxygen products to oxidize dihydrorhodamine in response to the phorbol ester PDBu (49). There was no difference in the ability of neutrophils (Fig. 8B) or monocytes (data not shown) from MRP-14$^{+/+}$ and MRP-14$^{-/-}$ mice to perform this activity. Preliminary experiments in which the kinetics of the oxidative burst were analyzed through oxidation of cytochrome *c* also revealed no differences between the two types of neutrophils (data not shown).

The ability of MRP-14$^{+/+}$ and MRP-14$^{-/-}$ myeloid cells to phagocytose FITC-labeled *E. coli* was tested. The occurrence and extent of phagocytosis by monocytes and neutrophils were evaluated by flow cytometry after quenching of extracellular bacterial fluorescence with trypan blue. Neutrophils were the major phagocytic population in freshly isolated bone marrow cells, but monocytes became phagocytic following 1 day of culture with interleukin-3 (data not shown). There was no difference between either neutrophils (Fig. 8C) or monocytes (data not shown) from MRP-14$^{+/+}$ and MRP-14$^{-/-}$ mice in uptake of FITC-*E. coli* or in the percentage of positive phagocytes over a time course ranging from 0 to 8 h.

Neutrophil apoptotic responses to the Ca^{2+} mobilizers ionomycin and thapsigargin were measured with LDS/DAPI staining and flow cytometric analysis. Cells were stimulated for up to 8 h with no clear difference in the proportions of live to apoptotic to dead cells between neutrophils (Fig. 8D) or monocytes (data not shown) of MRP-14$^{+/+}$ and MRP-14$^{-/-}$ mice for either of the stimuli. In addition, no differences were

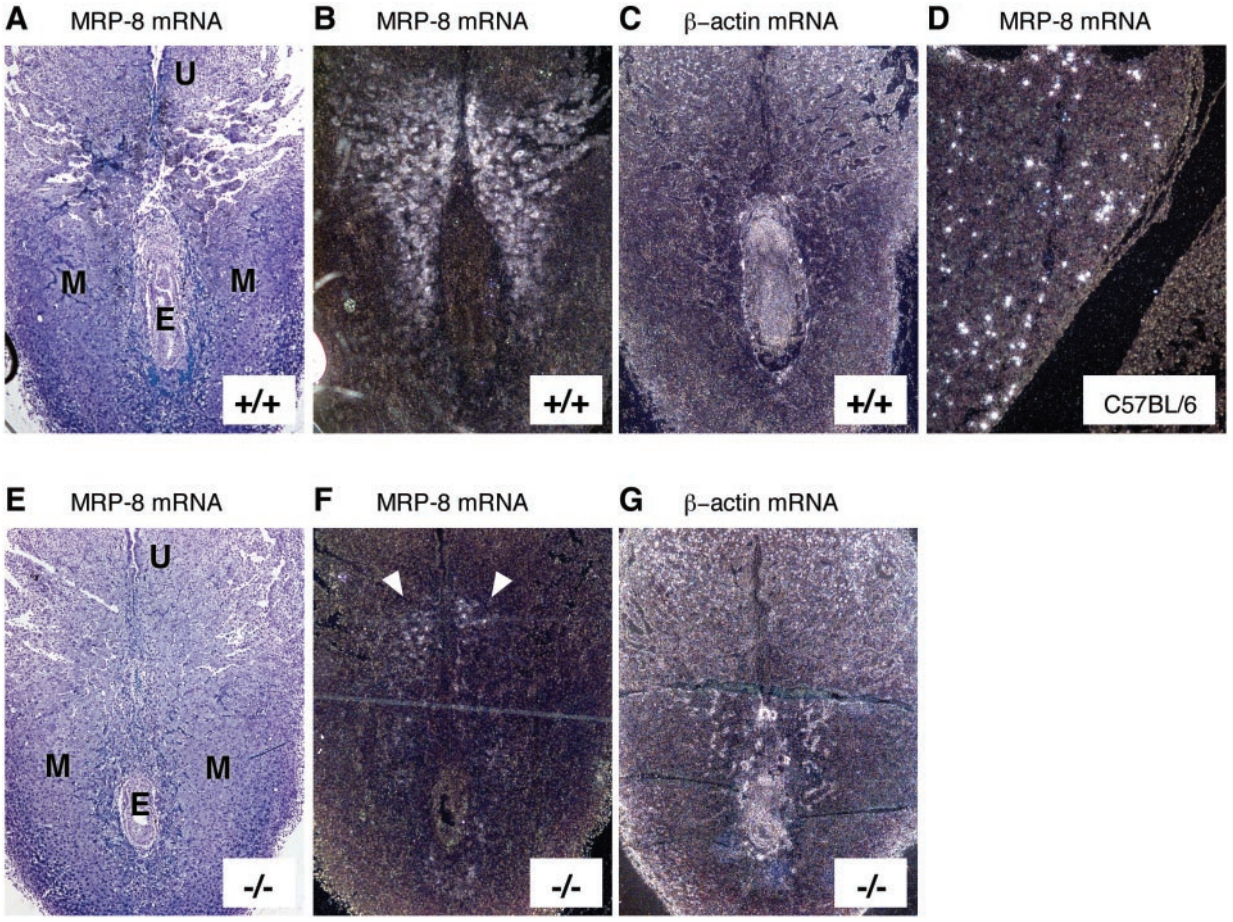

FIG. 5. Expression of *MRP-8* mRNA during embryonic development in MRP-14$^{-/-}$ mice at 7.5 d.p.c. In each longitudinal section, the remnant of the uterine lumen (U) is evident at the top of the section, with the developing embryo (E) visible below. Bright- and dark-field images of in situ hybridizations showing *MRP-8* mRNA expression in MRP-14$^{+/+}$ (A and B) and MRP-14$^{-/-}$ (E and F) (see arrows) tissues at 7.5 d.p.c. Hybridization with a β-actin probe was used as a positive control for embryonic and maternal expression in MRP-14$^{+/+}$ (C) and MRP-14$^{-/-}$ (G) tissues. The MRP-8 probe detected only myeloid cells in fetal liver during hematopoiesis at 14 d.p.c in a C57BL/6 embryo (D). MRP-14$^{+/+}$ and MRP-14$^{-/-}$ images are serial sections and are representative of six experiments. E, embryo; M, maternal tissue; U, remnant of uterine lumen.

seen with either gliotoxin, tumor necrosis factor alpha, or staurosporine-induced apoptosis (data not shown) or in spontaneous cell death in culture over several days (data not shown).

Response of MRP-14$^{-/-}$ mice to inflammatory stimulus. The ability of MRP-14$^{-/-}$ neutrophils and monocytes to mount an acute inflammatory response was tested in vivo with thioglycolate-induced peritonitis. Thioglycolate was injected intraperitoneally, and at selected time points, the elicited leukocytes were harvested, stained, and identified by flow cytometry. No significant difference was seen in the rate of either neutrophil (Fig. 9A) or monocyte (Fig. 9B) influx between MRP-14$^{+/+}$ and MRP-14$^{-/-}$ mice. Similar results were observed with the air pouch model in response to the inflammatory agent lipopolysaccharide (data not shown). We then examined the entry of other classes of leukocyte into the peritoneum over a longer time period in response to the stimulant thioglycolate. No difference was seen between MRP-14$^{+/+}$ and MRP-14$^{-/-}$ mice in the number of elicited eosinophils, B cells, or CD4 or CD8 T cells (Fig. 9C).

DISCUSSION

In this study, we characterized mice that were deficient in the S100 protein MRP-14 (S100A9). Although there was normal expression of *MRP-8* mRNA in the MRP-14$^{-/-}$ myeloid cells, surprisingly, no MRP-8 protein was present. The absence of MRP-8 protein could be due to inefficient translation of *MPR-8* mRNA or, more likely, due to instability of MRP-8 protein in the absence of its partner, MRP-14. This finding contrasts with evidence that murine MRP-14 and MRP-8 (CP-10) exist separately in myeloid cells (28, 40) and that CP-10 alone can function as a potent chemotactic factor (28, 29). In addition, immunohistochemical studies of mouse tissues show that MRP-14 (this study) and MRP-8 (data not shown) are coexpressed in myeloid cells. In support of this finding, the heterodimer can be isolated from spleen (data not shown) and bone marrow (13). Information from physical studies with the human proteins indicates that MRP-8 and MRP-14 form a heterodimer more readily than either forms a homodimer and that human MRP-8 in particular is unstable in the absence of

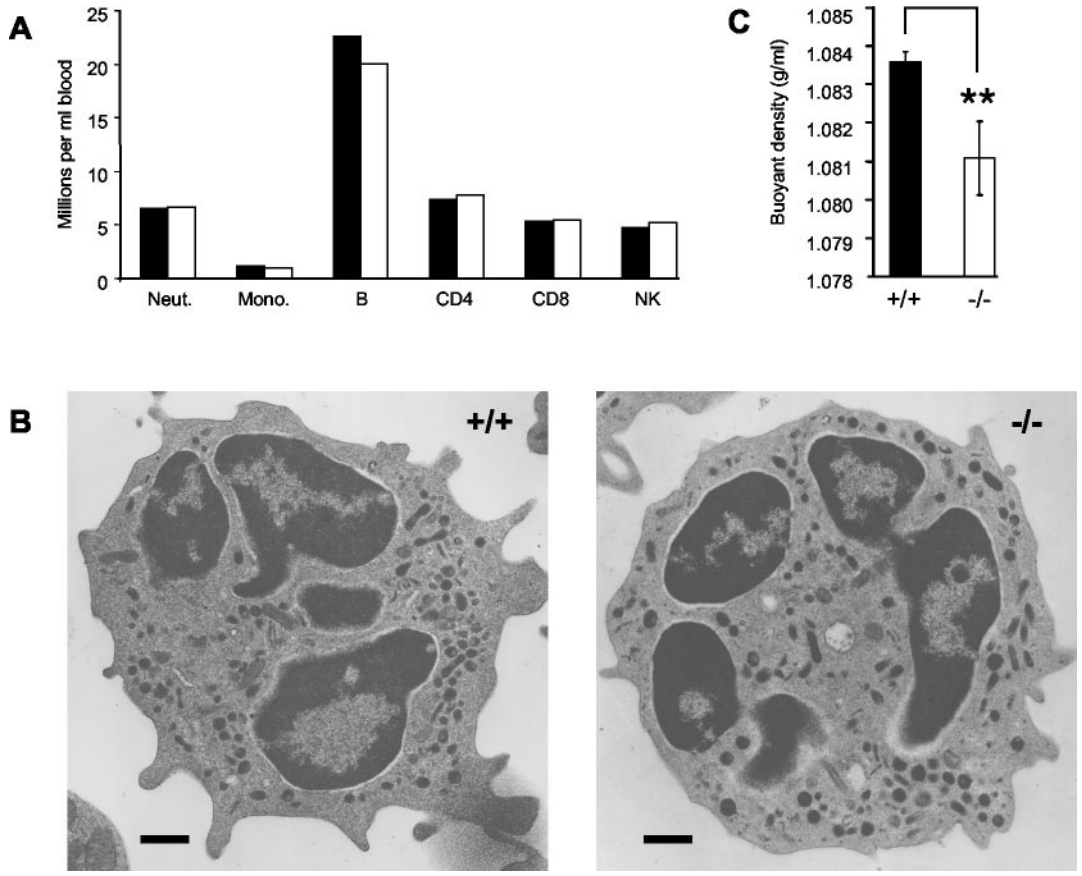

FIG. 6. Leukocyte numbers and myeloid cell architecture are unaltered but myeloid cells have a reduced density in MRP-14$^{-/-}$ mice. (A) Peripheral blood leukocytes were identified by flow cytometry: neutrophils (Neut.), monocytes (Mono.), B lymphocytes (B), CD4 and CD8 T lymphocytes, and natural killer cells (NK). An experiment representative of five is shown, with blood pooled from 11 MRP-14$^{+/+}$ and 9 MRP-14$^{-/-}$ mice. (B) Neutrophil ultrastructure is unchanged in MRP-14$^{-/-}$ mice. Transmission electron micrographs of isolated peripheral blood neutrophils; Scale bar, 500 nm; (C) Lack of MRP-14 results in reduced myeloid cell density. MRP-14$^{-/-}$ and MRP-14$^{+/+}$ bone marrow leukocytes were centrifuged on a continuous Percoll density gradient. A band containing 80% of the neutrophils loaded onto the gradient was significantly less dense in MRP-14$^{-/-}$ mice. Data, representative of five experiments, are expressed as mean ± standard deviation. **, $P < 0.001$.

human MRP-14 (24). This evidence suggests that MRP-8 and MRP-14 usually form a heterodimer in murine myeloid cells as they do in humans.

MRP-14$^{-/-}$ mice have normal organs and tissues and live a normal life span despite lacking both MRP-14 and MRP-8 proteins. This situation contrasts with MRP-8$^{-/-}$ mice, which die in utero (38). *MRP-8* mRNA has been reported to be expressed by cells surrounding the ectoplacental cone between 6.5 and 8.5 d.p.c. (38). In agreement with these findings, we show that *MRP-8* mRNA is expressed at 6.5 and 7.5 d.p.c. in MRP-14$^{+/+}$ and to a lesser extent in MRP-14$^{-/-}$ sections. Preliminary evidence indicates that MRP-8 protein is also expressed in this context (data not shown). Our observations conflict with those of Passey et al. in that we observed that *MRP-8* mRNA expression was associated with maternal decidual tissue rather than localized to the embryonic ectoplacental cone. However, the results suggest that in MRP-14$^{-/-}$ mice, MRP-8 can be expressed either alone or with a partner other than MRP-14. The nature of the cells expressing MRP-8 is presently unknown. These findings provide an explanation for why our MRP-14$^{-/-}$ mice are viable.

The lack of the MRP proteins had no effect on the number of tissue or circulating monocytes, neutrophils, lymphocytes, or NK cells or on myeloid cell numbers in lymphoid organs such as the spleen and bone marrow. The architecture of lymphoid tissues such as the spleen, where myeloid cells are easily detectable, was unaltered in MRP-14$^{-/-}$ mice. In humans, the MRP proteins are expressed constitutively by specific secretory epithelial tissues (19, 43) and hair follicles (46). In contrast, our immunohistochemical observations suggest that there is no similar constitutive staining of MRP proteins in murine epithelia (data not shown). However, other studies suggest that mRNAs for both MRP-14 and MRP-8 can be induced when skin is subjected to proinflammatory stress, such as wounding or phorbol ester treatment (12, 52).

In addition, several lines of evidence suggest that myeloid cells from the MRP-14$^{-/-}$ mice are equivalent in maturity to those from the MRP-14$^{+/+}$ mice. We detected no differences between MRP-14$^{+/+}$ and MRP-14$^{-/-}$ neutrophils in the expression of adhesion receptors (e.g., L-selectin and the integrins Mac-1, LFA-1, and $\alpha 4\beta 1$), constitutively or following activation with MIP-2, tumor necrosis factor alpha, or phorbol ester (data not shown). The loss of the MRP proteins also had no impact on the ultrastructure of the myeloid cells, as deter-

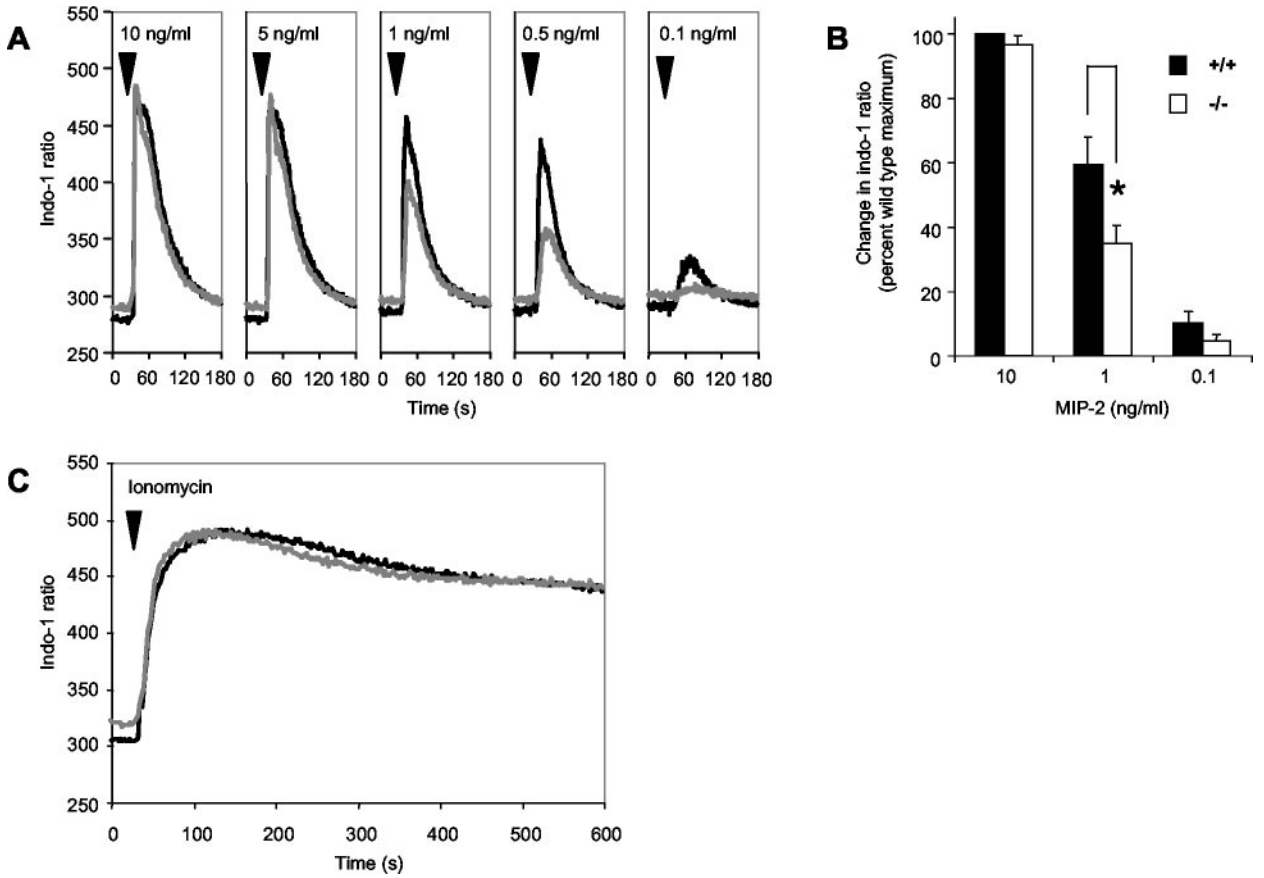

FIG. 7. Calcium flux responses in MRP-14$^{+/+}$ and MRP-14$^{-/-}$ neutrophils. (A) Bone marrow leukocytes were loaded with Indo-1, and neutrophils were identified by labeling with MAbs 7/4 and Gr-1. Intracellular calcium was monitored by flow cytometry and expressed as the ratio of the Indo-1 fluorescence at 424 nm and 530 nm. The median neutrophil–Indo-1 ratio of ≈500 to 700 events is plotted each second. MRP-14$^{-/-}$ (grey line) neutrophils were compared with MRP-14$^{+/+}$ (black line) cells at chemokine MIP-2 concentrations of 0.1 to 10 ng/ml. (B) Maximal changes in intracellular calcium levels induced by optimal concentrations of MIP-2 (10 ng/ml) were similar in MRP-14$^{+/+}$ and MRP-14$^{-/-}$ neutrophils, whereas those induced by suboptimal concentrations were significantly lower in MRP-14 null cells. Data are reported as mean ± standard error of the mean. *, $P < 0.05$. (C) Neutrophil calcium flux induced by 1 μM ionomycin.

mined by transmission electron microscopy, which is in keeping with the cytosolic localization of the proteins (9). However, the absence of the proteins results in a decrease in mean cellular density of 2.5 mg/ml in MRP-14$^{-/-}$ compared with MRP-14$^{+/+}$ neutrophils. This difference in density had no impact on the flow cytometric scatter properties (data not shown), confirming that neither the size nor the granularity of the cells was altered. The MRP proteins therefore have no role in either maintaining the cytoplasmic architecture of myeloid cells or determining their development or differentiation.

Murine MRP-14 protein is abundantly expressed, constituting 10 to 20% of neutrophil soluble protein (34). Similarly, human MRP-8/MRP-14 complex constitutes 45% of the cytosolic protein of neutrophils and ≈1% of monocytes (9). It might therefore be expected that the loss of MRP-14 and MRP-8 would be compensated for by an increase in other S100 proteins. Human myeloid cells also express S100A12, which is not complexed to MRP-8 or MRP-14 (43, 53). However, a search of murine genomic sequences indicates that the mouse does not possess an equivalent to the *S100A12* gene (data not shown). S100A4 is expressed in some murine leukocytes (15), and S100A1 is widely expressed in murine tissues (7), but expression of both was unaltered in MRP-14$^{-/-}$ bone marrow cells (data not shown). Studies of mice deficient in other S100 protein family members have also indicated the lack of compensatory increases in associated S100 family members. In *S100A1*$^{-/-}$ mice, cardiac cells do not upregulate S100 isoforms S100B, S100A4, and S100A11, which are coexpressed (7), and in *S100B*$^{-/-}$ mice, there is no compensatory upregulation of S100A1 or S100A6 (35). Similar to MRP-8 and MRP-14 in myeloid cells, S100A1 is expressed abundantly at ≈10 μM in left ventricular cardiomyocytes (7). Thus, it appears that myeloid and other cell types can develop and function reasonably normally in the absence of their distinctive S100 proteins.

As the MRP proteins have two EF hand Ca^{2+} binding motifs characteristic of the S100 protein family, an issue of importance was whether the myeloid cells from MRP-14$^{-/-}$ mice could maintain appropriate cellular levels of Ca^{2+} as well as generate normal Ca^{2+} fluxes. The basal level of intracellular Ca^{2+} in MRP-14$^{-/-}$ neutrophils was consistently higher than that of MRP-14$^{+/+}$ cells. Preliminary findings with Fluo-3-labeled bone marrow neutrophils demonstrated that basal levels of intracellular Ca^{2+} are 28 nM in MRP-14$^{+/+}$ cells and 36 nM in MRP-14$^{-/-}$ cells (data not shown). There was, however,

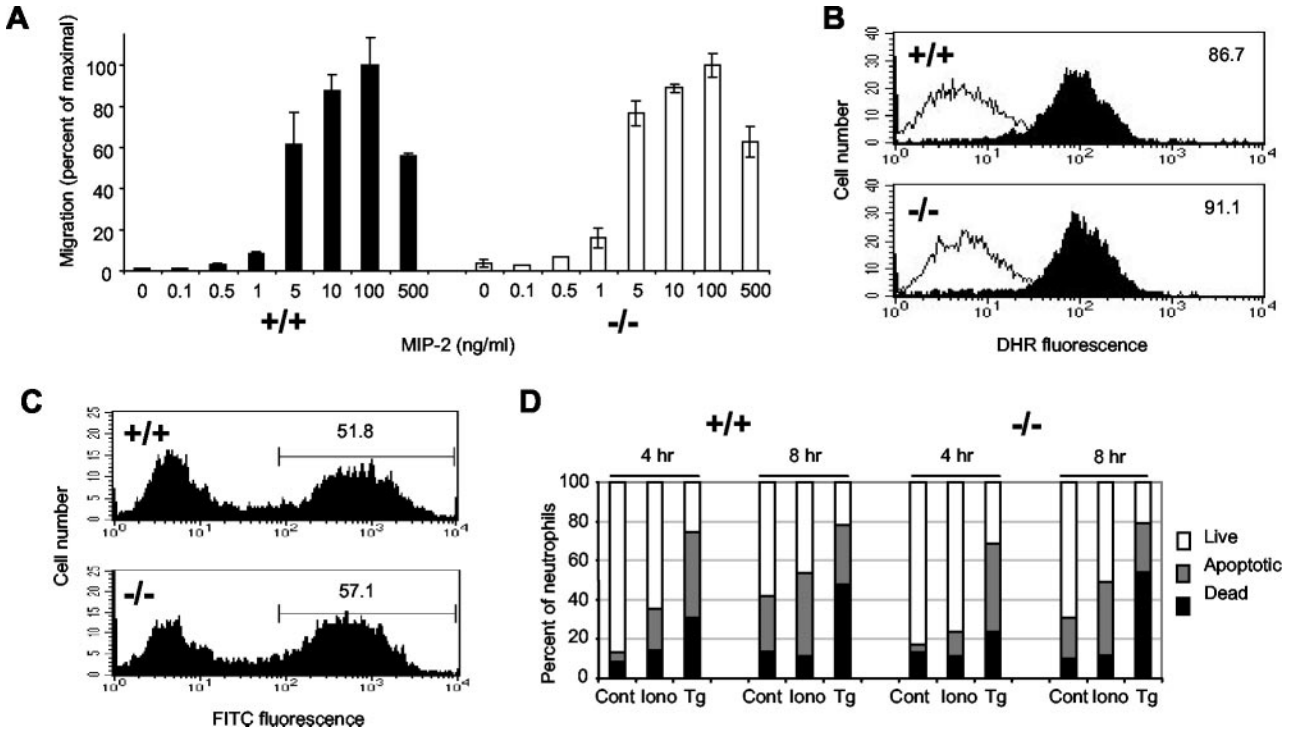

FIG. 8. Myeloid cell functions are normal in MRP-14$^{-/-}$ mice. (A) Chemotaxis of neutrophils in a Transwell assay in response to the chemokine MIP-2. Data are expressed as mean ± standard deviation, $n = 4$. (B) Dihydrorhodamine oxidation through induction of respiratory burst by neutrophils in response to 30 min of stimulation with the phorbol ester PDBu at 200 nM (solid histograms) or medium alone (empty histograms). Inset numbers show the dihydrorhodamine geometric mean fluorescence stimulation with PDBu, $n = 3$. (C) Phagocytosis of FITC-labeled *E. coli* by MRP-14$^{+/+}$ and MRP-14$^{-/-}$ neutrophils was determined by flow cytometry at 4 h. Inset numbers show the percentage of neutrophils containing fluorescent *E. coli* ($n = 3$). (D) Bone marrow neutrophil apoptosis induced by 1 μM ionomycin (Iono) and 2.5 μM thapsigargin (Tg) or medium alone (Cont) was determined by flow cytometry as described in the text after staining bone marrow cells with LDS and DAPI ($n = 4$).

no difference in the peak Ca^{2+} flux response generated to maximal levels of the neutrophil chemokine MIP-2 between MRP-14$^{-/-}$ and MRP-14$^{+/+}$ neutrophils. At suboptimal levels of MIP-2, the Ca^{2+} response in MRP-14$^{-/-}$ cells was diminished by ≈40% compared with that of MRP-14$^{+/+}$ cells. Furthermore, no differences were found in the calcium response of MRP-14$^{-/-}$ neutrophils generated by the Ca^{2+} ionophore ionomycin or the intracellular Ca^{2+} mobilizer thapsigargin in the presence or absence of extracellular calcium. This suggests that calcium release from intracellular stores and calcium-induced calcium entry across the plasma membrane are functioning normally in MRP-14$^{-/-}$ cells.

In summary, these observations are consistent with the interpretation that MRP-8 and MRP-14 act as Ca^{2+} sensors during Ca^{2+} responses and may enhance the Ca^{2+} signal generated by suboptimal levels of chemokine. Further evidence that MRP-8 and MRP-14 are acting as calcium sensors comes from physical studies demonstrating conformational changes following Ca^{2+} binding by the complex (24). In addition, analysis of the crystal structures of S100A6 (37) and S100B (6) in the presence and absence of Ca^{2+} shows conformational change in the S100 dimer, leading to the exposure of a hydrophobic patch which provides a docking site for interaction with other proteins on each monomer, thereby propagating the Ca^{2+} signal. There are now a number of situations where such Ca^{2+}-induced changes in S100 proteins have been demonstrated to have biological relevance. For example, S100B inhibits p53 phosphorylation by protein kinase C in a Ca^{2+}-dependent fashion (1). The giant kinase twitchin is activated by S100A1 in a Ca^{2+}- and Zn^{2+}-dependent manner (16). S100β activates photoreceptor guanylate cyclase (8) and also the nuclear Ndr serine/threonine kinase with dependence on Ca^{2+} (33).

Ca^{2+} binding affinities have yet to be measured for MRP-8 and MRP-14, but other S100 proteins bind Ca^{2+} in the micro- to millimolar range (17). An issue of interest is how MRP-8 and MRP-14 and other S100 proteins might be involved in the normal calcium signaling activities of cells and how their affinities for calcium may be modulated. Several S100 proteins, including MRP-14, bind Zn^{2+} (40, 44), which can increase the affinity for Ca^{2+} (2, 17), potentially by modulating the variant EF hand loop (4). In addition, intracellular conditions such as association with certain binding partners may favor conformational changes leading to higher Ca^{2+} binding affinities.

A most relevant issue is whether myeloid cell function is dependent upon the Ca^{2+} binding activity of MRP-8 and MRP-14. Neutrophils are the first cells at sites of tissue injury, closely followed by monocytes. Many key neutrophil functions have been documented to require Ca^{2+} (39), and it was therefore unexpected that there was no difference in numerous functions of either monocytes or neutrophils from MRP-14$^{-/-}$ mice compared with those from MRP-14$^{+/+}$ mice. It was par-

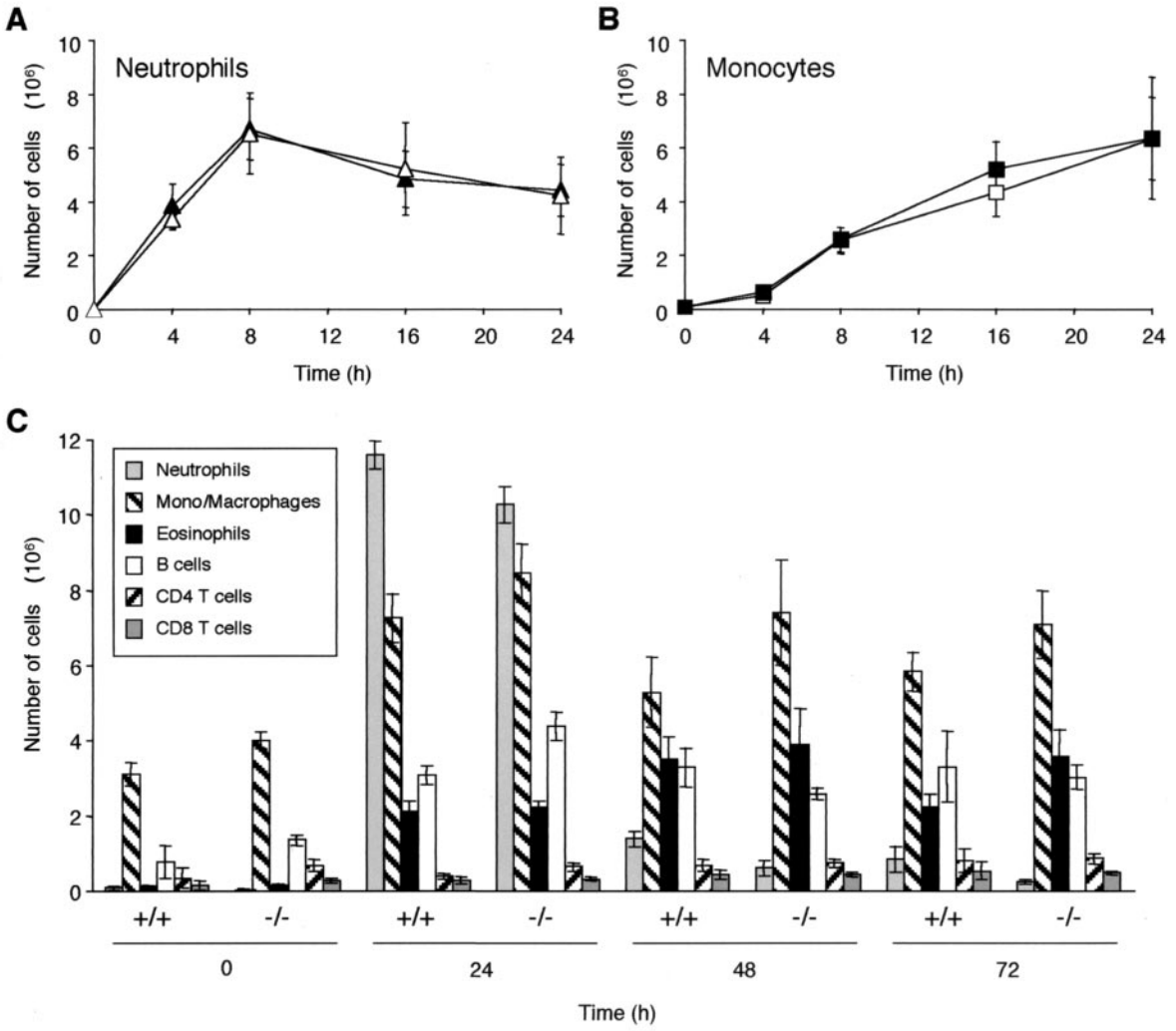

FIG. 9. Migration of myeloid cells into the peritoneum after thioglycolate injection. (A and B) Solid symbols, MRP-14$^{+/+}$; open symbols, MRP-14$^{-/-}$. (C) Migration of various classes of leukocyte into the peritoneum after thioglycolate injection up to 72 h. These data are representative of three experiments which utilized six to eight MRP-14$^{+/+}$ and MRP-14$^{-/-}$ mice per time point for each experiment. Data are reported as mean ± standard error of the mean.

ticularly of interest that the diminished level of Ca^{2+} response to suboptimal levels of the chemokine MIP-2 in MRP-14$^{-/-}$ neutrophils had no impact on their chemotactic response to MIP-2. Furthermore, Ca^{2+} dysregulation is an important factor leading to cell apoptosis (3), and it seemed a reasonable speculation that the MRP proteins might act to stabilize Ca^{2+} levels in myeloid cells under apoptosis-inducing conditions. However, no difference was observed in the rate of either apoptosis or cell death in neutrophils and monocytes of MRP-14$^{-/-}$ versus MRP-14$^{+/+}$ mice.

As in vitro assays never fully reproduce the situation in vivo, it was anticipated that the response to an inflammatory signal or to an infection might reveal a difference between the MRP-14$^{+/+}$ and MRP-14$^{-/-}$ mice. Surprisingly, analysis of the responses of neutrophils, monocytes, and other leukocytes to thioglycolate-induced peritonitis over a 72-h time course showed no difference in the ability of MRP-14$^{-/-}$ and MRP-14$^{+/+}$ mice to respond to this challenge. The response to *Leishmania donovani* is now recognized to be dependent on Gr-1-positive leukocytes, potentially neutrophils (48). Preliminary results show no effect of MRP-14 deletion on the early response to *L. donovani* (P. Kaye, personal communication). In summary, these results suggest that MRP-14 and MRP-8 do not have a general function in myeloid cell development or in the proinflammatory responses of these cells. A search is presently under way for further models where the lack of these abundant proteins might have substantial impact.

ACKNOWLEDGMENTS

J.H., R.M., and K.T. contributed equally to this study.

We are extremely grateful to the following colleagues for their participation in this project: Florian Otto and Ian Rosewell for guidance and assistance in the generation of the MRP-14$^{-/-}$ mice; Francisco Nicolas for essential help with the RNase protection assay; Barbara Turner, Georgina Corden, Julie Bee, and Gill Hutchinson for maintenance of the mice and critical assistance with the experimental protocols; Jane Steele for MAb production; Nicola O'Reilly and Dave

Frith for two-dimensional gel analysis; Carol Upton for TEM; George Elia for immunohistochemisry; Richard Poulsom and Rosemary Jeffery for the in situ hybridization study; and Bradley Spencer-Dene for help with embryo preparation. We thank our colleagues Alison McDowall, Katherine Giles, Andrew Smith, and Facundo Batista for helpful comments on the manuscript.

K.T. was supported by funds from Upjohn Pharmacia. The work was supported by the Cancer Research UK London Research Institute (formerly Imperial Cancer Research Fund).

REFERENCES

1. **Baudier, J., C. Delphin, D. Grunwald, S. Khochbin, and J. J. Lawrence.** 1992. Characterization of the tumor suppressor protein p53 as a protein kinase C substrate and a S100b-binding protein. Proc. Natl. Acad. Sci. USA **89:**11627–11631.
2. **Baudier, J., N. Glasser, and D. Gerard.** 1986. Ions binding to S100 proteins. I. Calcium- and zinc-binding properties of bovine brain S100αα, S100a (αβ), and S100b (ββ) protein: Zn^{2+} regulates Ca^{2+} binding on S100b protein. J. Biol. Chem. **261:**8192–8203.
3. **Berridge, M. J., P. Lipp, and M. D. Bootman.** 2000. The versatility and universality of calcium signalling. Nat. Rev. Mol. Cell. Biol. **1:**11–21.
4. **Brodersen, D. E., J. Nyborg, and M. Kjeldgaard.** 1999. Zinc-binding site of an S100 protein revealed. Two crystal structures of Ca^{2+}-bound human psoriasin (S100A7) in the Zn^{2+}-loaded and Zn^{2+}-free states. Biochemistry **38:**1695–1704.
5. **Donato, R.** 2001. S100: a multigenic family of calcium-modulated proteins of the EF-hand type with intracellular and extracellular functional roles. Int. J. Biochem. Cell. Biol. **33:**637–668.
6. **Drohat, A. C., D. M. Baldisseri, R. R. Rustandi, and D. J. Weber.** 1998. Solution structure of calcium-bound rat S100B(ββ) as determined by nuclear magnetic resonance spectroscopy. Biochemistry **37:**2729–2740.
7. **Du, X. J., T. J. Cole, N. Tenis, X. M. Gao, F. Kontgen, B. E. Kemp, and J. Heierhorst.** 2002. Impaired cardiac contractility response to hemodynamic stress in S100A1-deficient mice. Mol. Cell. Biol. **22:**2821–2829.
8. **Duda, T., K. W. Koch, V. Venkataraman, C. Lange, M. Beyermann, and R. K. Sharma.** 2002. Ca(2+) sensor S100β-modulated sites of membrane guanylate cyclase in the photoreceptor-bipolar synapse. EMBO J. **21:**2547–2556.
9. **Edgeworth, J., M. Gorman, R. Bennett, P. Freemont, and N. Hogg.** 1991. Identification of p8,14 as a highly abundant heterodimeric calcium binding protein complex of myeloid cells. J. Biol. Chem. **266:**7706–7713.
10. **Freemont, P., N. Hogg, and J. Edgeworth.** 1989. Sequence identity. Nature **339:**516.
11. **Gabrielsen, T. O., I. Dale, P. Brandtzaeg, P. S. Hoel, M. K. Fagerhol, T. E. Larsen, and P. O. Thune.** 1986. Epidermal and dermal distribution of a myelomonocytic antigen (L1) shared by epithelial cells in various inflammatory skin diseases. J. Am. Acad. Dermatol. **15:**173–179.
12. **Gebhardt, C., U. Breitenbach, J. P. Tuckermann, K. H. Richter, and P. Angel.** 2002. Calgranulins S100A8 and S100A9 are negatively regulated by glucocorticoid in a c-Fos-dependent manner and overexpressed throughout skin carcinogenesis. Oncogene **21:**4266–4276.
13. **Goebeler, M., J. Roth, U. Henseleit, C. Sunderkotter, and C. Sorg.** 1993. Expression and complex assembly of calcium-binding proteins MRP8 and MRP14 during differentiation of murine myelomonocytic cells. J. Leukoc. Biol. **53:**11–18.
14. **Gribenko, A. V., J. E. Hopper, and G. I. Makhatadze.** 2001. Molecular characterization and tissue distribution of a novel member of the S100 family of EF-hand proteins. Biochemistry **40:**15538–15548.
15. **Grigorian, M., E. Tulchinsky, O. Burrone, S. Tarabykina, G. Georgiev, and E. Lukanidin.** 1994. Modulation of *mts1* expression in mouse and human normal and tumor cells. Electrophoresis **15:**463–468.
16. **Heierhorst, J., B. Kobe, S. C. Feil, M. W. Parker, G. M. Benian, K. R. Weiss, and B. E. Kemp.** 1996. Ca^{2+}/S100 regulation of giant protein kinases. Nature **380:**636–639.
17. **Heizmann, C. W., and J. A. Cox.** 1998. New perspectives on S100 proteins: a multi-functional Ca^{2+}-, Zn^{2+}-, and Cu^{2+}-binding protein family. Biometals **11:**383–397.
18. **Henderson, R. B., L. H. Lim, P. A. Tessier, F. N. Gavins, M. Mathies, M. Perretti, and N. Hogg.** 2001. The use of lymphocyte function-associated antigen (LFA)-1-deficient mice to determine the role of LFA-1, Mac-1, and α4 integrin in the inflammatory response of neutrophils. J. Exp. Med. **194:** 219–226.
19. **Hessian, P. A., J. Edgeworth, and N. Hogg.** 1993. MRP-8 and MRP-14, two abundant Ca^{2+}-binding proteins of neutrophils and monocytes. J. Leukoc. Biol. **53:**197–204.
20. **Hofmann, M. A., S. Drury, C. Fu, W. Qu, A. Taguchi, Y. Lu, C. Avila, N. Kambham, A. Bierhaus, P. Nawroth, M. F. Neurath, T. Slattery, D. Beach, J. McClary, M. Nagashima, J. Morser, D. Stern, and A. M. Schmidt.** 1999. RAGE mediates a novel proinflammatory axis: a central cell surface receptor for S100/calgranulin polypeptides. Cell **97:**889–901.
21. **Hogg, N., C. Allen, and J. Edgeworth.** 1989. Monoclonal antibody 5.5 reacts with p8,14, a myeloid molecule associated with some vascular endothelium. Eur. J. Immunol. **19:**1053–1061.
22. **Howell, M., and C. S. Hill.** 1997. XSmad2 directly activates the activin-inducible, dorsal mesoderm gene XFKH1 in *Xenopus* embryos. EMBO J. **16:**7411–7421.
23. **Hubl, W., J. Iturraspe, G. A. Martinez, C. E. Hutcheson, C. G. Roberts, D. D. Fisk, M. W. Sugrue, J. R. Wingard, and R. C. Braylan.** 1998. Measurement of absolute concentration and viability of CD34+ cells in cord blood and cord blood products with fluorescent beads and cyanine nucleic acid dyes. Cytometry **34:**121–127.
24. **Hunter, M. J., and W. J. Chazin.** 1998. High level expression and dimer characterization of the S100 EF-hand proteins, migration inhibitory factor-related proteins 8 and 14. J. Biol. Chem. **273:**12427–12435.
25. **Jinquan, T., H. Vorum, C. G. Larsen, P. Madsen, H. H. Rasmussen, B. Gesser, M. Etzerodt, B. Honore, J. E. Celis, and K. Thestrup-Pedersen.** 1996. Psoriasin: a novel chemotactic protein. J. Investig. Dermatol. **107:**5–10.
26. **Kerkhoff, C., C. Sorg, N. N. Tandon, and W. Nacken.** 2001. Interaction of S100A8/S100A9-arachidonic acid complexes with the scavenger receptor CD36 may facilitate fatty acid uptake by endothelial cells. Biochemistry **40:**241–248.
27. **Komada, T., R. Araki, K. Nakatani, I. Yada, M. Naka, and T. Tanaka.** 1996. Novel specific chemotactic receptor for S100L protein on guinea pig eosinophils. Biochem. Biophys. Res. Commun. **220:**871–874.
28. **Lackmann, M., C. J. Cornish, R. J. Simpson, R. L. Moritz, and C. L. Geczy.** 1992. Purification and structural analysis of a murine chemotactic cytokine (CP-10) with sequence homology to S100 proteins. J. Biol. Chem. **267:**7499–7504.
29. **Lackmann, M., P. Rajasekariah, S. E. Iismaa, G. Jones, C. J. Cornish, S. Hu, R. J. Simpson, R. L. Moritz, and C. L. Geczy.** 1993. Identification of a chemotactic domain of the pro-inflammatory S100 protein CP-10. J. Immunol. **150:**2981–2991.
30. **Lagasse, E., and R. G. Clerc.** 1988. Cloning and expression of two human genes encoding calcium-binding proteins that are regulated during myeloid differentiation. Mol. Cell. Biol. **8:**2402–2410.
31. **Lagasse, E., and I. L. Weissman.** 1992. Mouse MRP8 and MRP14, two intracellular calcium-binding proteins associated with the development of the myeloid lineage. Blood **79:**1907–1915.
32. **McColl, S. R., and P. H. Naccache.** 1997. Calcium mobilization assays. Methods Enzymol. **288:**301–309.
33. **Millward, T. A., C. W. Heizmann, B. W. Schafer, and B. A. Hemmings.** 1998. Calcium regulation of Ndr protein kinase mediated by S100 calcium-binding proteins. EMBO J. **17:**5913–5922.
34. **Nacken, W., C. Sopalla, C. Propper, C. Sorg, and C. Kerkhoff.** 2000. Biochemical characterization of the murine S100A9 (MRP14) protein suggests that it is functionally equivalent to its human counterpart despite its low degree of sequence homology. Eur. J. Biochem. **267:**560–565.
35. **Nishiyama, H., T. Knopfel, S. Endo, and S. Itohara.** 2002. Glial protein S100B modulates long-term neuronal synaptic plasticity. Proc. Natl. Acad. Sci. USA **99:**4037–4042.
36. **Odink, K., N. Cerletti, J. Bruggen, R. G. Clerc, L. Tarcsay, G. Zwadlo, G. Gerhards, R. Schlegel, and C. Sorg.** 1987. Two calcium-binding proteins in infiltrate macrophages of rheumatoid arthritis. Nature **330:**80–82.
37. **Otterbein, L. R., J. Kordowska, C. Witte-Hoffmann, C. L. Wang, and R. Dominguez.** 2002. Crystal structures of S100A6 in the Ca^{2+}-free and Ca^{2+}-bound states. The calcium sensor mechanism of S100 proteins revealed at atomic resolution. Structure (Cambridge) **10:**557–567.
38. **Passey, R. J., E. Williams, A. M. Lichanska, C. Wells, S. Hu, C. L. Geczy, M. H. Little, and D. A. Hume.** 1999. A null mutation in the inflammation-associated S100 protein S100A8 causes early resorption of the mouse embryo. J. Immunol. **163:**2209–2216.
39. **Pettit, E. J., E. V. Davies, and M. B. Hallett.** 1997. The microanatomy of calcium stores in human neutrophils: relationship of structure to function. Histol. Histopathol. **12:**479–490.
40. **Raftery, M. J., C. A. Harrison, P. Alewood, A. Jones, and C. L. Geczy.** 1996. Isolation of the murine S100 protein MRP14 (14 kDa migration-inhibitory-factor-related protein) from activated spleen cells: characterization of post-translational modifications and zinc binding. Biochem. J. **316:**285–293.
41. **Rammes, A., J. Roth, M. Goebeler, M. Klempt, M. Hartmann, and C. Sorg.** 1997. Myeloid-related protein (MRP) 8 and MRP14, calcium-binding proteins of the S100 family, are secreted by activated monocytes via a novel, tubulin-dependent pathway. J. Biol. Chem. **272:**9496–9502.
42. **Ridinger, K., E. C. Ilg, F. K. Niggli, C. W. Heizmann, and B. W. Schafer.** 1998. Clustered organization of S100 genes in human and mouse. Biochim. Biophys. Acta **1448:**254–263.
43. **Robinson, M. J., and N. Hogg.** 2000. A comparison of human S100A12 with MRP-14 (S100A9). Biochem. Biophys. Res. Commun. **275:**865–870.
44. **Robinson, M. J., P. Tessier, R. Poulsom, and N. Hogg.** 2002. The S100 family heterodimer, MRP-8 and MRP-14, binds with high affinity to heparin and heparan sulfate glycosaminoglycans on endothelial cells. J. Biol. Chem. **277:** 3658–3665.
45. **Schafer, B. W., and C. W. Heizmann.** 1996. The S100 family of EF-hand

calcium-binding proteins: functions and pathology. Trends Biochem. Sci. **21:**134–140.
46. **Schmidt, M., R. Gillitzer, A. Toksoy, E. B. Brocker, U. R. Rapp, R. Paus, J. Roth, S. Ludwig, and M. Goebeler.** 2001. Selective expression of calcium-binding proteins S100a8 and S100a9 at distinct sites of hair follicles. J. Investig. Dermatol. **117:**748–750.
47. **Senior, P. V., D. R. Critchley, F. Beck, R. A. Walker, and J. M. Varley.** 1988. The localization of laminin mRNA and protein in the postimplantation embryo and placenta of the mouse: an in situ hybridization and immunocytochemical study. Development **104:**431–446.
48. **Smelt, S. C., S. E. Cotterell, C. R. Engwerda, and P. M. Kaye.** 2000. B cell-deficient mice are highly resistant to *Leishmania donovani* infection, but develop neutrophil-mediated tissue pathology. J. Immunol. **164:**3681–3688.
49. **Smith, J. A., and M. J. Weidemann.** 1993. Further characterization of the neutrophil oxidative burst by flow cytometry. J. Immunol. Methods **162:**261–268.
50. **Srikrishna, G., K. Panneerselvam, V. Westphal, V. Abraham, A. Varki, and H. H. Freeze.** 2001. Two proteins modulating transendothelial migration of leukocytes recognize novel carboxylated glycans on endothelial cells. J. Immunol. **166:**4678–4688.
51. **Teigelkamp, S., R. S. Bhardwaj, J. Roth, G. Meinardus-Hager, M. Karas, and C. Sorg.** 1991. Calcium-dependent complex assembly of the myeloic differentiation proteins MRP-8 and MRP-14. J. Biol. Chem. **266:**13462–13467.
52. **Thorey, I. S., J. Roth, J. Regenbogen, J. P. Halle, M. Bittner, T. Vogl, S. Kaesler, P. Bugnon, B. Reitmaier, S. Durka, A. Graf, M. Wockner, N. Rieger, A. Konstantinow, E. Wolf, A. Goppelt, and S. Werner.** 2001. The Ca^{2+}-binding proteins S100A8 and S100A9 are encoded by novel injury-regulated genes. J. Biol. Chem. **276:**35818–35825.
53. **Vogl, T., C. Propper, M. Hartmann, A. Strey, K. Strupat, C. van den Bos, C. Sorg, and J. Roth.** 1999. S100A12 is expressed exclusively by granulocytes and acts independently from MRP8 and MRP14. J. Biol. Chem. **274:**25291–25296.
54. **Wan, C. P., C. S. Park, and B. H. Lau.** 1993. A rapid and simple microfluorometric phagocytosis assay. J. Immunol. Methods **162:**1–7.
55. **Witko-Sarsat, V., P. Rieu, B. Descamps-Latscha, P. Lesavre, and L. Halbwachs-Mecarelli.** 2000. Neutrophils: molecules, functions and pathophysiological aspects. Lab. Investig. **80:**617–653.